Energy Engineering

Tech Science Press

Doi:10.32604/ee.2025.073405

ARTICLE

Parameter Adaptive SVIC FR Strategy for Doubly-Fed Induction Generators Considering Wind Condition Zoning

Li Sun, Fanjun Zeng, Hongbo Liu, Chenglian Ma*, Qiting Zhang and Jingzhou Zhu

Key Laboratory of Modern Power System Simulation and Control & Renewable Energy Technology, Ministry of Education, Northeast Electric Power University, Jilin, 132012, China

*Corresponding Author: Chenglian Ma. Email: machenglian@neepu.edu.cn

Received: 17 September 2025; Accepted: 21 November 2025; Published: 06 August 2026

ABSTRACT: The widespread integration of large-scale wind power has resulted in decreased equivalent inertia in power systems, thereby compromising their frequency regulation (FR) capabilities. Conventional synthetic inertia control faces challenges under stochastic wind conditions, including inadequate utilization of rotor kinetic energy in high wind condition regions and the risk of triggering rotor speed stability limits in low wind condition regions. To overcome these limitations, in this paper, a parameter adaptive synthetic virtual inertial control (SVIC) framework based on wind speed partition is proposed. The control mechanisms are designed differently across partitioned wind condition intervals: in high-wind-speed zones, a simplified fuzzy rule set dynamically optimizes the virtual inertia and droop coefficients (K_d and K_p), enhancing performance by aggressively yet safely utilizing the rotor's stored energy within a predefined secure speed range. Conversely, under low-wind conditions, an adaptive attenuation mechanism safeguards rotor speed by scaling down these coefficients. Simulation results demonstrate that the proposed strategy effectively balances FR efficacy and operational security under stochastic wind conditions. It achieves improvement in the frequency nadir while constraining rotor speed fluctuations within safe limits, thereby providing substantial support for enhancing system frequency stability.

KEYWORDS: Synthetic virtual inertia control; doubly-fed induction generator; fuzzy logic control; wind condition zoning; over-speed de-loading

1 Introduction

Against the backdrop of promoting the "Two Replacements" strategy and achieving the "Dual Carbon" goals, the global energy landscape is undergoing a profound shift, with renewables becoming a central component of power system planning and operation [1,2]. Within the renewable energy sector, wind power demonstrates significant potential for expansion, owing to its distinct advantages in terms of accessibility, cost-effectiveness, and technological maturity. However, as wind power penetration continues to increase, it will further undermine the system's disturbance resistance and FR capability [3,4]. To tackle the challenge of system inertia reduction due to high wind power penetration, Grid Codes issued by various countries explicitly mandate that grid-connected wind turbines must provide inertia and primary FR capabilities [5].

Currently, wind turbine capabilities for FR are primarily achieved through either auxiliary control loops that modify their active power output or energy storage systems that compensate for a power imbalance during frequency disturbances [6]. These approaches primarily include power reserve control [7,8], SVIC

[9–11] and supplementary energy storage modules [12,13]. Among these, SVIC operates through the controlled release of the rotor's kinetic energy via deliberate speed modulation. This approach not only enables the delivery of additional active power to the grid but also provides rapid inertial support to mitigate further frequency decline. Owing to its superior economic efficiency, SVIC has emerged as the predominant FR strategy for modern wind power systems. Reference [14] pioneered the SVIC strategy, enabling wind turbines to participate in grid FR by harnessing the kinetic energy of their rotating masses. Reference [15] proposes a segmented setting of the droop coefficient, using a large coefficient initially for rapid response and gradually reducing it later to avoid excessive release of rotor kinetic energy. However, conventional fixed-parameter SVIC struggles to adapt to dynamic wind condition variations. Under high wind conditions, it results in insufficient utilization of rotor kinetic energy, while during low wind periods, excessive energy release may trigger rotor speed excursions beyond safety limits. Building upon this foundation, reference [16] proposes an adaptive control method based on fuzzy logic, which dynamically adjusts the power tracking curve according to frequency deviation and its rate of change. However, its fuzzy rules do not fully account for the influence of wind speed, resulting in limited adaptability under complex wind conditions. Reference [17] employs the whale optimization algorithm to optimize system output, which enhances overall performance. However, the control structure is complex and fails to fundamentally resolve the inherent contradictions of wind turbines across different wind speed ranges. Reference [18] proposes a full-wind-speed range adaptive SVIC based on fuzzy logic. This control enhances the wind turbine's ability to participate in system FR. However, the single fuzzy controller requires more conservative fuzzy rules at low wind conditions to ensure rotor speed security, which limits the turbine's performance; at high wind conditions, the complex fuzzy rule base imposes a greater computational burden during fuzzy inference. Reference [19] focuses on the inherent contradiction between the turbine's innate speed controller and the SVIC, proposing to mitigate this conflict by adjusting the speed controller parameters via fuzzy reasoning. However, this reference has some shortcomings: the control logic is complex, and it does not consider the impact of different wind speed conditions on the inherent contradiction. Reference [20] recognizes the conflict between the speed controller and the FR loop and employs fuzzy control to dynamically adjust the speed controller parameters. However, the inputs to the fuzzy controller in this reference are only the system frequency deviation and RoCoF, without considering that the FR capability of the wind turbine varies under different wind conditions. Reference [21] proposes combining over-speed de-loading with SVIC to provide reserve capacity and inertia support. However, the SVIC part in this literature uses fixed parameters, unable to adapt to dynamically changing wind conditions and system frequency states. Reference [22] adopts wind turbine overspeed control and considers blade fatigue load analysis, but the control parameters are fixed and do not account for the randomness of wind speed.

In summary, the common limitation of existing methods lies in their attempt to "apply a single strategy to all wind scenarios". To overcome this limitation, this paper, for the first time, constructs a hybrid adaptive control framework based on wind speed zoning, namely, the collaborative control of wind speed zones. This framework intelligently identifies the operating zone (high kinetic energy zone/low kinetic energy zone) in which the wind turbine is currently operating and activates distinctly different, optimized control algorithms, achieving a systematic "divide-and-conquer" solution. In the high-speed zone, the core issue is how to fully and intelligently utilize the abundant rotor kinetic energy. To this end, this paper introduces "simplified fuzzy rules". Compared to computationally intensive full-wind-speed fuzzy rules, these rules are specifically optimized for the high-speed zone, enabling dynamic adjustment of control parameters with minimal computational cost and precisely unlocking the potential for virtual inertia support. In the low-speed zone, the core challenge shifts to ensuring absolute rotor speed safety while providing limited support. Traditional fuzzy logic, due to its uncertainty, poses a risk of instability in this zone. Therefore, this paper designs a "new exponential decay function". It provides a deterministic, continuous, and adaptive safety boundary, allowing the control intensity to smoothly decay with wind speed, fundamentally eliminating the risk of rotor speed exceeding limits—a feat difficult to achieve with fuzzy rules. This approach enhances power reserve capacity, achieving coordinated optimization of FR performance and operational security for DFIG across the entire wind conditions spectrum.

2 Operational Characteristics of DFIG and Over-Speed De-Loading Frequency Control

With the growing integration of wind power, the dynamic characteristics of DFIGs play an increasingly critical role in power system frequency stability. This chapter focuses on the core operational mechanisms of DFIGs, aiming to establish a theoretical foundation for their participation in system FR control.

2.1 Mathematical Model and Operational Principles of Wind Turbines

$$\begin{cases} P_{\mathrm{m}} = 0.5\pi\rho C_{\mathrm{P}}\left(\lambda,\beta\right) r_{\mathrm{w}}^{2} v_{\mathrm{w}}^{3} \\ C_{\mathrm{P}} = 0.22\left(\dfrac{116}{\lambda_{\mathrm{i}}} - 0.4\beta - 5\right) e^{\dfrac{-12.5}{\lambda_{\mathrm{i}}}} \\ \dfrac{1}{\lambda_{i}} = \dfrac{1}{\lambda + 0.08} - \dfrac{0.035}{\beta^{3}+1} \\ \lambda = \dfrac{r_{\mathrm{w}} w_{\mathrm{r}}}{v_{\mathrm{w}}} \end{cases}, \tag{1}$$

in Eq. (1), ρ denotes the air density, $C_{\mathrm{p}}(\lambda,\beta)$ represents the dimensionless power coefficient, r_{w} is the rotor radius, and v_{w} denotes the wind velocity. Under steady wind conditions, the turbine's output power depends exclusively on the power coefficient.

As derived from Eq. (1), the wind turbine's output is highly sensitive to the power coefficient $C_{\mathrm{p}}(\lambda,\beta)$, which varies with tip-speed ratio and blade pitch angle. The corresponding power coefficient C_{p} curve is depicted in Fig. 1.

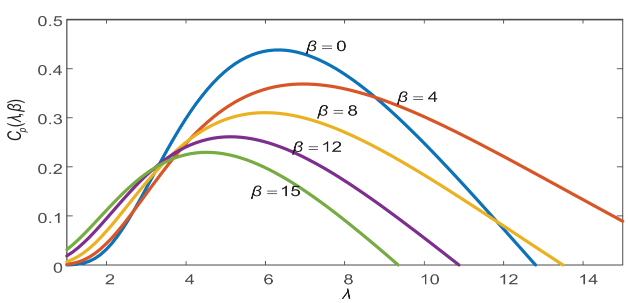

Figure 1: C_{p} characteristic curve

2.2 Principles of Additional Rotor Over-Speed De-Loading Control for DFIGs

Under standard operating conditions, DFIGs follow the Maximum Power Point Tracking (MPPT) strategy, which inherently offers no power reserve capacity. Consequently, upward power regulation becomes infeasible, preventing bidirectional FR. To address this limitation, de-loading operation via pitch angle control or rotor over-speed control can be implemented [23,24]. These strategies enable DFIGs to maintain a certain level of power reserve, thereby facilitating their participation in frequency support services. Pitch angle control adjusts the blade orientation to minimize wind energy loss while increasing wind power input, enabling turbine operation at a sub-maximum power point with reserved capacity. However, this method relies on specific mechanical components, and frequent pitch angle adjustments may accelerate mechanical wear. Additionally, it is only applicable in high-wind-speed regions.

Considering the above reasons, this paper employs rotor overspeed control to achieve de-loading operation of wind turbines. The underlying principle is illustrated in Fig. 2. Here, ω_{n} represents the rated wind condition of the turbine, Point A denotes the maximum power point operation, where the rotor velocity is ω_{opt} and the output active power is P_{opt}. By accelerating the rotor to the reference velocity ω_{re}, the turbine operates at point B, delivering an output active power of P_{re}, thereby maintaining a certain power reserve.

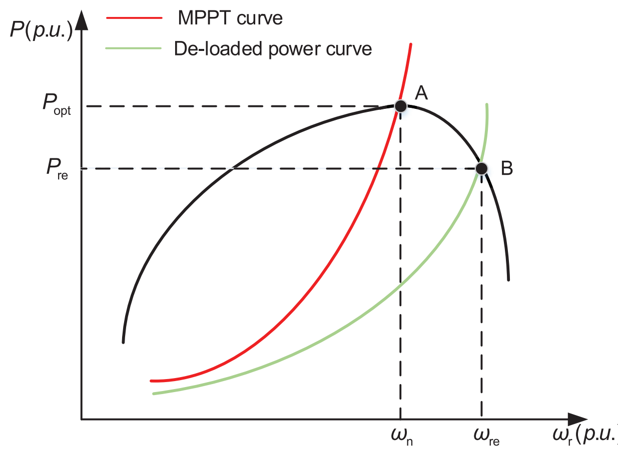

Figure 2: Over-speed de-loading and MPPT operational characteristics

3 Analysis of Principles of Traditional SVIC for Wind Turbines

The supplementary SVIC facilitates wind turbine participation in system FR by utilizing the available kinetic energy in the rotor, thereby augmenting active power injection. Given the finite amount of kinetic energy stored in the rotor, it is essential to optimize its utilization through time-dependent parameter adjustments during different phases of frequency response. This section begins with an analysis of inertia in thermal-wind power systems, and then introduces the SVIC method. However, the fixed control coefficients in conventional methods restrict the extent to which wind turbines can contribute to FR. Therefore, this paper proposes a parameter-adaptive SVIC method of FR for DFIGs on the basis of wind condition zoning.

3.1 Analysis of Inertia Impact Factors in Thermal-Wind Power Systems

Conventional generation units deliver power to the grid while simultaneously providing inherent inertia through their rotating components. In contrast, wind turbines interfaced with the grid through power converters lack inherent inertial response capabilities as a result of the decoupling introduced by power electronics. This results in systems operating in low-inertia mode, increasing vulnerability to frequency disturbances. To mitigate the low-inertia phenomenon in power systems and harness the potential of leveraging kinetic energy from wind turbines' rotor for FR, SVIC is implemented, allowing wind turbines to deliver synthetic inertia support to the grid.

The inertia time constant is conventionally used to quantify system inertia in contemporary electrical networks. For conventional generation units, this constant is defined as shown in Eq. (2):

$$H = \frac{\sum_{j=1}^{n} \frac{J_j \omega_e^2}{2p_j^2}}{\sum_{j=1}^{n} S_{N,j}}, \tag{2}$$

in the equation, J denotes the angular mass ($kg \cdot m^2$), ω represents the angular velocity (rad/s), and S refers to the rated capacity (VA).

Owing to the decoupling introduced by power electronics, they cannot respond to grid frequency variations by adjusting rotor speed in the same manner as conventional thermal units. The inertia time constant for thermal-wind integrated power systems is expressed in Eq. (3) as follows:

$$H_{W.T} = \frac{\sum_{j=1}^{n} \frac{J_j \omega_e^2}{2p_j^2}}{\sum_{j=1}^{n} S_{N,j} + \sum_{i=1}^{m} S_{w,i}}, \tag{3}$$

where S_w denotes the rated capacity, m denotes the total count of wind turbines.

As indicated in Eq. (3), increased wind power penetration reduces the system inertia, thereby degrading power system stability.

When supplementary SVIC is activated in wind turbines, rotor speed modulation facilitates the release of kinetic energy, thereby altering the active power output. The corresponding change in kinetic energy E is expressed in Eq. (4) as follows:

$$\Delta E_W = \frac{J_{W,vir}}{2p_W^2 S_{W,i}} \left[(\omega_{e0} + \Delta\omega_e)^2 - \omega_{e0}^2 \right], \tag{4}$$

where $J_{W,vir}$ represents the virtual moment of inertia of the wind turbine, while ω_{e0} and $\Delta\omega_{e0}$ denote the initial electrical angular velocity and its increment, respectively.

Based on the preceding formulation, the implementation of SVIC in wind turbines augments the power system's equivalent inertia time constant, which is given by Eq. (5) as follows:

$$H_W = \frac{\sum_{j=1}^{n} \frac{J_j \omega_e^2}{2p_j^2} + \sum_{i=1}^{n} \frac{J_{W,vir} \omega_e^2}{2p_{W,i}^2}}{\sum_{j=1}^{n} S_{N,j} + \sum_{i=1}^{m} S_{w,i}}, \tag{5}$$

as indicated in Eq. (5), the system equivalent inertia increases with the addition of SVIC to wind turbines, and the grid frequency can be effectively regulated by adjusting the virtual moment of inertia of the turbines.

3.2 Influencing Factors of Traditional SVIC

SVIC typically combines virtual inertia control and droop control into an integrated control strategy. When a power deficit occurs in the system, this approach adds a proportional-derivative (PD) control loop to the rotor side. By decelerating the turbine rotor releases its stored kinetic energy, resulting in an increase in active power output to help offset the system power deficit. The supplementary active power ΔP_W is mathematically expressed in Eq. (6) as follows:

$$\Delta P_W = -\left(2H_W \frac{d\Delta f_W}{dt} + D_W \Delta f_W\right) = -\left(K_d \frac{d\Delta f_W}{dt} + K_p \Delta f_W\right), \tag{6}$$

in the equation, H_W denotes the equivalent inertia time constant contributed by the wind turbine through SVIC, D_W represents the primary FR coefficient, Δf_W refers to the power contribution from the wind farm during frequency disturbances, and K_d and K_p are the differential and proportional control coefficients of the SVIC, respectively.

The actual active power output of the DFIG is formulated in Eq. (7):

$$P_e = P_{del} + \Delta P_W, \tag{7}$$

the dynamic response equation of the system frequency is described by Eq. (8) [25]:

$$2\left(H_{W.T} + H_{W.vir}\right) \frac{d\Delta f}{dt} = P_m - P_L + P_e - \left(D_{W.T} + D_{W.vir}\right) \Delta f, \tag{8}$$

consequently, wind turbines can rapidly respond to system frequency variations through an additional PD control loop, thereby exhibiting characteristics similar to synchronous generators. The SVIC strategy is illustrated in Fig. 3.

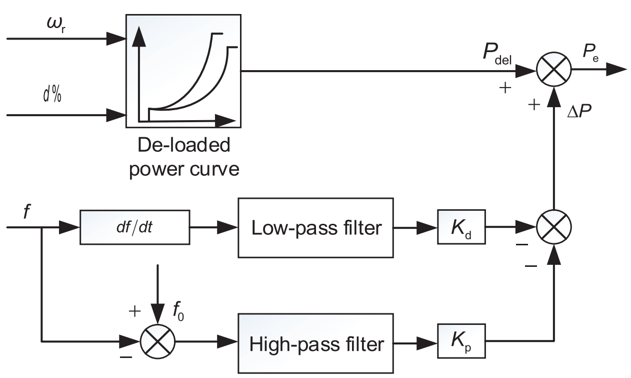

Figure 3: Block diagram of SVIC for primary FR

When SVIC is applied, wind turbines release kinetic energy stored in their rotors to respond to system frequency variations. The extent of kinetic energy extraction depends on the values of parameters K_p and K_d in the control formula. However, it should be noted that larger damping and equivalent inertia are not always better for system performance. Although increased damping and equivalent inertia help prevent further frequency decline during frequency drops, excessive values can impede frequency recovery during the restoration process. This may prevent the system from rapidly returning to the secure frequency range and consequently reduce the system's readiness for subsequent frequency disturbances. Therefore, the values of K_p and K_d should be carefully configured to achieve optimal performance.

As shown in Fig. 4, when K_p is held constant, a larger K_d parameter elevates the frequency nadir following a disturbance. However, as the system approaches the frequency nadir, the RoCoF diminishes significantly. At this stage, it is common practice to reduce the K_d parameter to prevent excessive release of rotor kinetic energy. When K_d is held constant, a larger K_p parameter results in a relatively unchanged rate of change of frequency (RoCoF) but elevates the frequency nadir following a disturbance. However, as the

K_p parameter increases, the severity of the second frequency drop (SFD) becomes more pronounced. This occurs because a higher K_p value enables the wind turbine to utilize more kinetic energy from the rotor for primary FR. Consequently, upon exiting the frequency support mode, the resulting power imbalance in the system increases, thereby exacerbating the SFD. Therefore, as the system approaches the frequency nadir, it is common practice to reduce the K_p parameter to prevent excessive release of rotor kinetic energy.

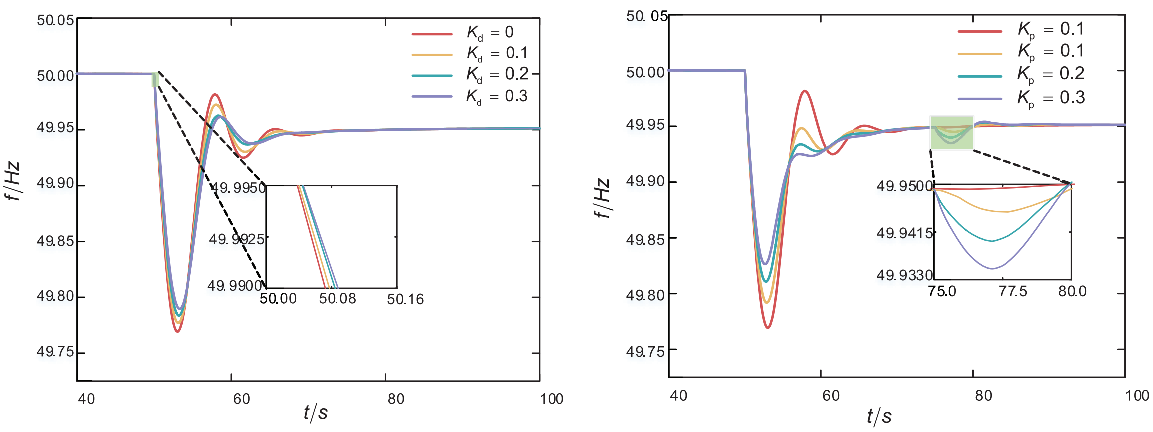

(**a**) (**b**)

Figure 4: Frequency response curves under different control parameters. (**a**) different K_d parameters (**b**) different K_p parameters

However, in traditional SVIC, once the values of K_p and K_d are predetermined, they remain immutable during operation.

4 Parameter-Adaptive SVIC Based on Wind Condition Zoning

Concurrently, the prevailing wind conditions within the wind farm govern the available kinetic energy in the turbine rotors, which in turn determines their capacity to support system FR. Simultaneously, the wind condition in the wind farm directly affects the kinetic energy reserve of the turbine rotors, thereby impacting their ability to contribute to system FR. Considering these factors, this paper adopts a zoning-based control strategy segmented by wind condition intervals. In regions with high wind conditions, the rotor retains ample kinetic energy, enabling full utilization of the turbines' FR potential. In low wind condition zones, where the rotational kinetic energy reserve is limited, the FR strategy prioritizes operational safety while balancing it with the turbines' FR capacity. The wind condition zoning results are illustrated in Fig. 5.

4.1 Fuzzy Logic-Based Variable-Coefficient SVIC

For wind turbines utilizing SVIC, their effectiveness in FR is predominantly governed by K_d and K_p. Fixed values of these coefficients struggle to balance the trade-off between FR capability and post-regulation rotor speed recovery. To dynamically adjust of K_d and K_p, this paper adopts a fuzzy inference system (FIS) for real-time parameter optimization. Traditional SVIC strategies based on fuzzy logic typically use only frequency deviation and RoCoF as inputs to the fuzzy inference system. However, variations in wind conditions directly determine the operational conditions of wind turbines and the available rotor kinetic energy reserve. The SVIC strategy requires real-time adaptation of its control parameters in response to varying wind conditions. Therefore, this paper specifically incorporates the influence of wind conditions as a key input to the fuzzy inference system.

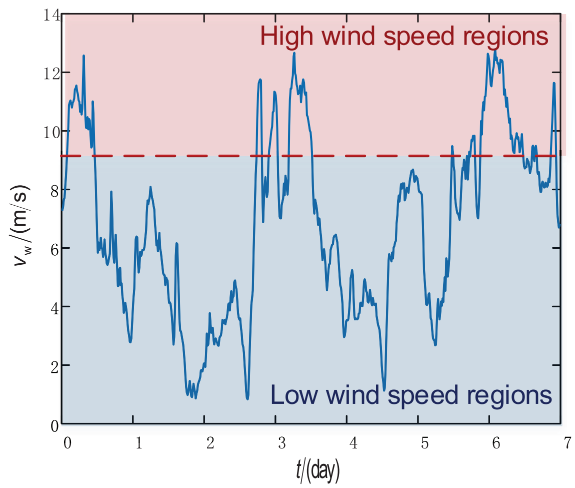

Figure 5: Stochastic wind condition scenario

As shown in Fig. 6, in the FIS, the input variables are the system's RoCoF, frequency deviation, and wind condition. The wind condition includes three fuzzy subsets: {RB, M, RS}. The Δf and $\mathrm{d}f/\mathrm{d}t$ (RoCoF) involve five fuzzy subsets: {NV, NM, ZM, PM, PV}. These inputs collectively determine the adjustment of the frequency response. The output variables are the parameters of K_d and K_p. The parameters of K_d and K_p comprise five fuzzy subsets: {NT, ST, ZM, MH, PH}. The FIS utilizes triangular membership functions and the centroid method for defuzzification. The membership functions are illustrated in Fig. 7.

If a variable-coefficient SVIC based on fuzzy logic is adopted across the entire wind condition range, the rule-based design may lead to unsmooth transitions between intervals, resulting in discontinuous additional active power from wind turbines, which can further cause irregularities in the frequency improvement curve. Moreover, setting up a comprehensive rule base for the full wind condition range requires a large computational burden. However, during high wind conditions, wind turbines possess sufficient rotor kinetic energy reserves, making them suitable for participating in system FR through variable-coefficient SVIC with larger fuzzy rules. Considering the above factors, this paper proposes a fuzzy logic-based variable-coefficient SVIC with streamlined fuzzy rules under high wind conditions. By simplifying the fuzzy rules and reducing the computational burden, fuzzy rules are set to maximize the release of rotational kinetic energy for system FR, thereby improving system frequency stability.

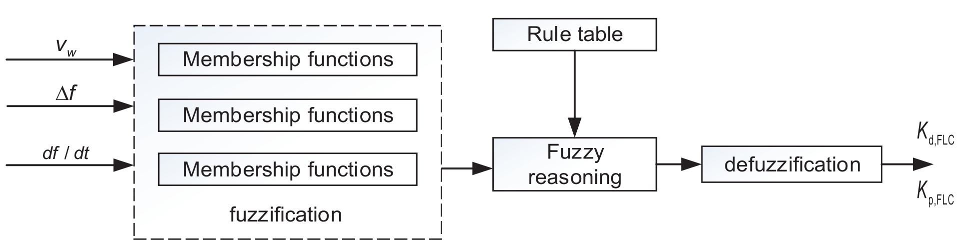

Figure 6: Fuzzy Logic Controller (FLC) structure

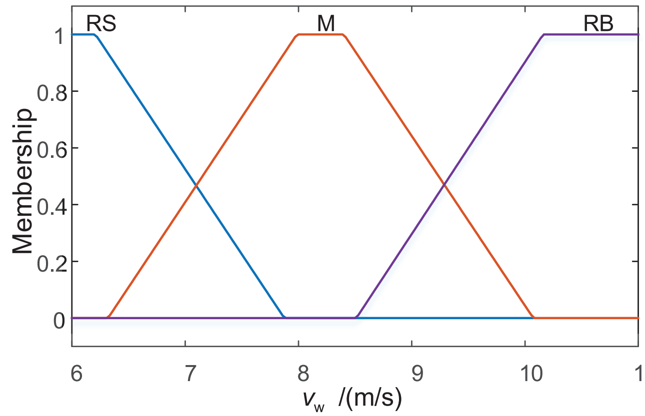

(**a**)

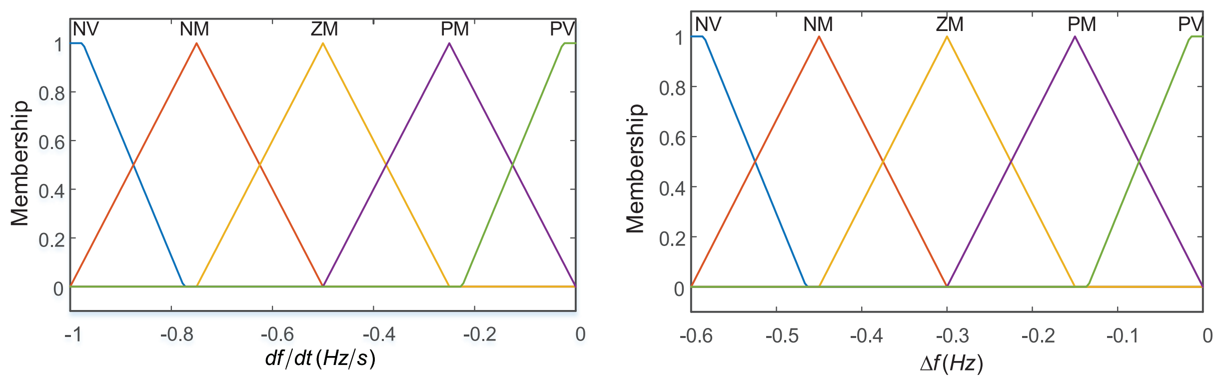

(**b**)

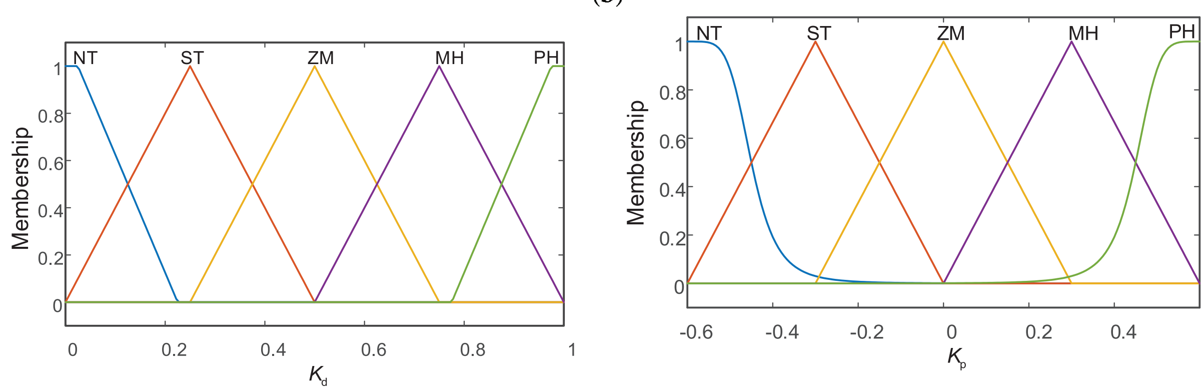

(**c**)

Figure 7: Membership function. (**a**) FIS input: wind condition. (**b**) FIS input variables. (**c**) FIS output variables

Based on practical conditions, the virtual inertia rules derived from FIS inference according to the system's RoCoF and frequency deviation are presented in Table 1, while the droop control rules are shown in Table 2.

Table 1: Simplified virtual inertia control coefficient rule table

$K_{\mathrm{d,FLC}}$		Δf				
v_{w}	$\mathrm{d}f/\mathrm{d}t$	**NV**	**NM**	**ZM**	**PM**	**PV**
	NV	PH	PH	PH	PH	PH
	NM	PH	PH	PH	PH	PM
RB	ZM	PM	PM	PM	ZM	ZM
	PM	ST	ST	ST	ST	ST
	PV	ST	ST	NT	NT	NT

Table 2: Simplified droop control coefficient rule table

$K_{\mathrm{p,FLC}}$		Δf				
v_{w}	$\mathrm{d}f/\mathrm{d}t$	**NV**	**NM**	**ZM**	**PM**	**PV**
	NV	NT	NT	NT	NT	NT
	NM	NT	NT	NT	ST	ST
RB	ZM	ST	ST	ZM	ZM	ZM
	PM	ZM	MH	MH	MH	MH
	PV	MH	MH	PH	PH	PH

According to the established fuzzy rules and membership functions, the defuzzification process is carried out through the fuzzy inferencer to obtain the fuzzy-inferred virtual inertia control coefficient and droop control coefficient, as shown in Fig. 8.

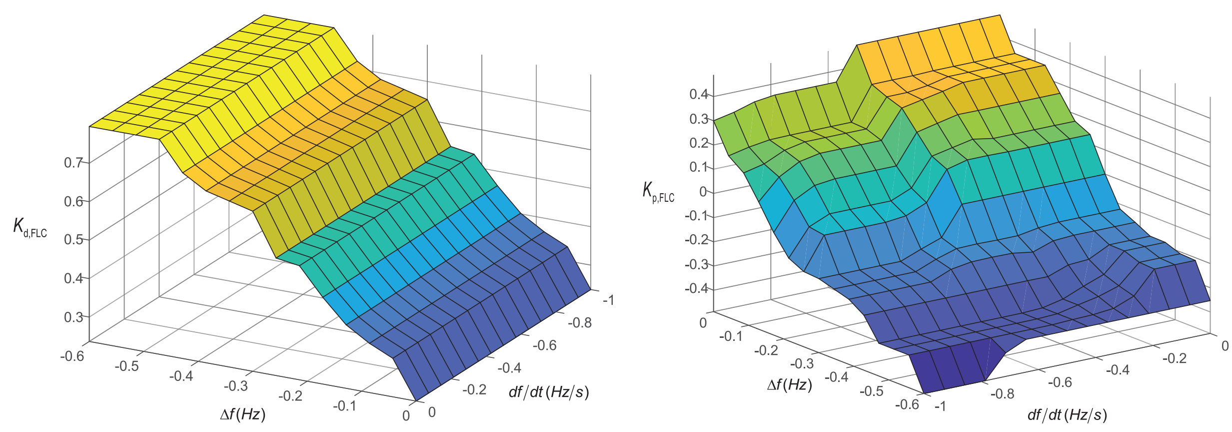

(**a**) (**b**)

Figure 8: The outputs of the FIS. (**a**) denotes the value of K_{d}. (**b**) represents the value of Δf

The underlying principle of the FIS is as follows: at the inception of a grid frequency event, when the Δf is relatively small while the $\mathrm{d}f/\mathrm{d}t$ is large, the inferred K_{d} is supposed to be configured to a higher value to utilize the limited rotor kinetic energy to counteract rapid frequency changes. Conversely, when the Δf

is significant but the $\mathrm{d}f/\mathrm{d}t$ slows, the inferred K_p is supposed to be configured to a higher parameter to improve the frequency nadir.

It is crucial to note that the objective of maximizing energy utilization in the high-wind-speed zone is pursued under the strict constraint of the rotor speed's lower limit. The simplified fuzzy rules are designed to output high control coefficients only during the initial stage of frequency drop when the rotor speed is sufficiently high. As the rotor speed decreases and approaches the safe threshold, the inherent reduction of RoCoF will, in turn, guide the fuzzy inference system to automatically lower the control coefficients according to its rule base (e.g., see Table 1, where low RoCoF states correspond to lower K_d values). This dynamic adjustment inherently prevents the rotor speed from exceeding its minimum allowable value.

4.2 Wind Conditions-Decay Function-Based Variable-Coefficient SVIC

When wind turbines operate under low wind conditions, the constant control coefficients of traditional SVIC can easily lead to safety issues such as rotor speed exceeding limits. Although fuzzy control possesses a certain degree of adaptive capability, its reasoning process may still output large inertia support commands, resulting in excessively rapid depletion of rotor kinetic energy and causing speed instability or even grid disconnection. If the fuzzy control rules are improperly designed, overly conservative control strategies often fail to adequately exploit the rotor's stored kinetic energy, resulting in unsatisfactory FR performance. To address the above issues, this paper proposes a variable-coefficient SVIC based on a decay function that responds to wind condition variations. The decay function enables continuous and monotonic reduction of the synthetic inertia coefficient according to wind conditions, achieving more refined power regulation and better aligning with the dynamic response requirements of this operational range.

When the measured wind velocity v_w falls under the predefined threshold v_m, the comprehensive inertia control coefficients are designed to attenuate in accordance with the wind condition, as described by the following Eq. (9):

$$\begin{cases} K_\mathrm{dlow} = K_\mathrm{d} \times \left(1 - e^{-\alpha}\right) \\ \alpha = v_\mathrm{w}/v_\mathrm{m} \end{cases}, \tag{9}$$

in the equation, K_d represents the SVIC coefficient, K_dlow denotes the wind-speed-attenuated SVIC coefficient proposed in this paper, v_w is the actual wind condition, and v_m represents the rated wind condition of the wind turbine.

The decay function we proposed, $K_\mathrm{dlow} = K_\mathrm{d} \times (1 - e^{-v_\mathrm{w}/v_\mathrm{m}})$, was selected based on the following control system design principles:

(1) The function $f(a) = 1 - e^{-a}$ satisfies $f(0) = 0$, when $a = 0$ (i.e., $v_\mathrm{w} = 0$). This means the virtual inertia coefficient decays completely to zero under windless conditions, ensuring the wind turbine provides no inertial support and guaranteeing absolute rotor safety. When $a = 1$ (i.e., $v_\mathrm{w} = v_\mathrm{m}$), $f(1) = 1 - e^{-1} \approx 0.632$. This means the inertia coefficient recovers to approximately 63.2% of its original value at the rated wind speed, enabling a smooth transition to the fuzzy control mode used in the high wind speed zone.

(2) The function is continuous and monotonically increasing. This ensures that changes in the control coefficient do not cause abrupt transitions, which is beneficial for system stability.

(3) As wind speed increases, the coefficient increases smoothly and non-linearly. This trend aligns with the increase in the available kinetic energy of the wind turbine. Although kinetic energy is proportional to the square of the wind speed, the exponential decay form provides more conservative attenuation

in the low wind speed region, ensuring safety at very low wind speeds, while allowing appropriate support in the medium-to-low wind speed range.

The wind-speed-adaptive SVIC coefficient ensures that the rotor speed remains within safe limits when DFIGs participate in system FR, thereby guaranteeing operational security. The overall control logic structure proposed in this study for the full wind condition range is illustrated in Fig. 9. The mathematical formulas reflected in the control strategy are shown in Eq. (10).

$$\begin{cases} P_e = P_{del} + \left(-K_{d,FLC}\dfrac{df}{dt} - K_{p,FLC}\Delta f\right), (v_w > v_t) \\ P_e = P_{del} + \left(-K_{dlow}\dfrac{df}{dt} - K_{plow}\Delta f\right), (v_w < v_t) \end{cases} \tag{10}$$

In this paper, the DFIGs participate in system FR through an additional frequency control strategy. The control logic uses whether the wind condition exceeds the threshold wind condition as the decision condition. When the wind condition is higher than the threshold, the DFIGs employ an auxiliary parameter-adaptive SVIC based on fuzzy logic, coordinated with over-speed de-loading control. When the wind condition is lower than the threshold, the DFIGs adopt an auxiliary parameter-adaptive SVIC based on a decay function, with the same coordination mechanism.

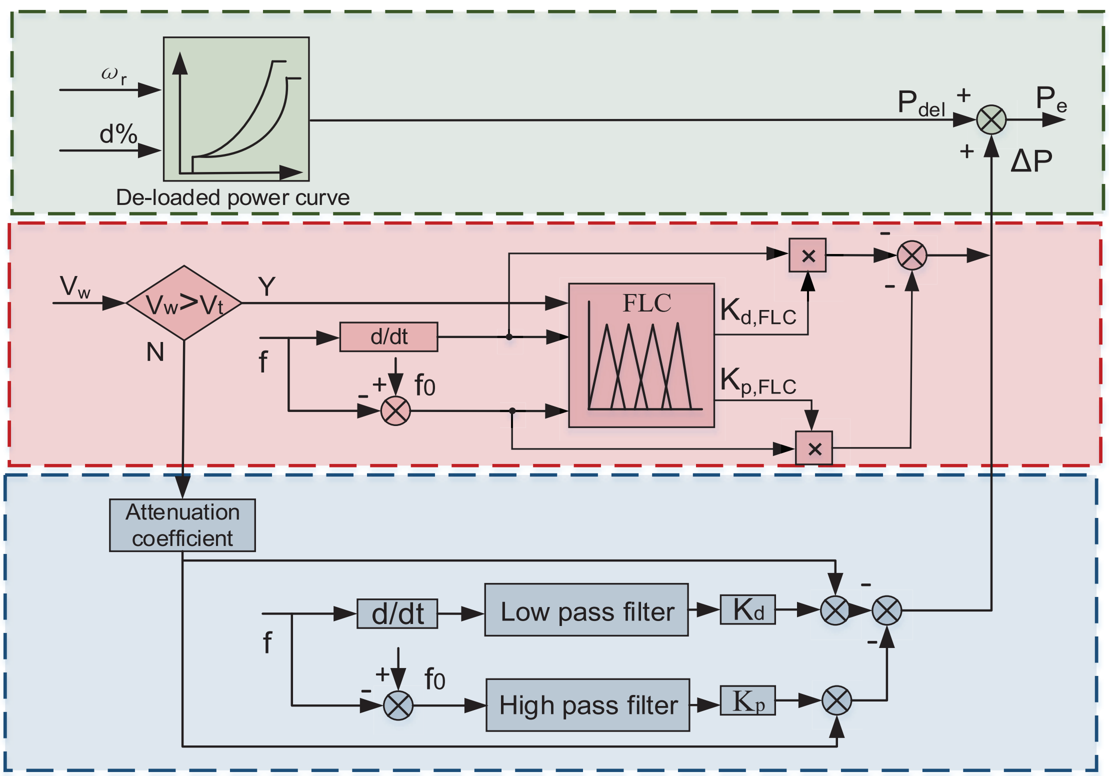

Figure 9: Block diagram of SVIC and over-speed control under stochastic wind scenarios

5 Case Study Validation

To validate the performance and practicality of the proposed control strategy, a simulation model was developed using the MATLAB/Simulink environment, adopting the IEEE three-machine nine-bus system as shown in Fig. 10. The strategy proposed in this paper was compared with three other control strategies.

Among them, synchronous generators G1 and G2 each have an installed capacity of 100 MW, the wind farm comprises thirty-five 2 MW wind turbines, yielding a total installed capacity of 70 MW, and the wind power penetration rate is 25.9%. The active power output of the synchronous generator and the DFIG, as well as the active power demand of each load, are shown in Table 3. The internal parameters of the DFIG and the mechanical parameters of the synchronous generator are presented in Table 4.

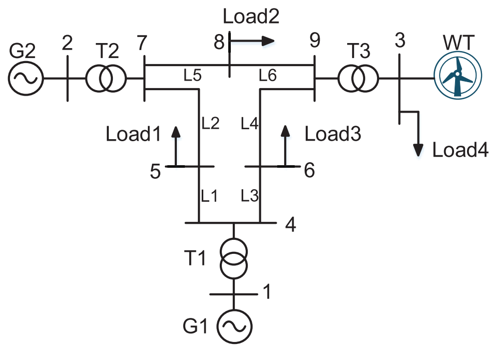

Figure 10: System topology diagram

Table 3: Generator active power output and load active power demand

Type	P_N/MW	Type	P_N/MW
Synchronous Generators 1	100	Load1	117
Synchronous Generators 2	100	Load2	35
DFIGs	35*2	Load3	95
Load4	2.5		

Table 4: Parameters of each generator and load

Parameter name of DFIG	Values and units	Parameter name of SG	Values and units
Power factor	0.95	Power factor	0.85
H	5.04 s	H(SG1)	23.64 s
v_N	10 m/s	H(SG2)	6.4 s
K_d	0.3 pu	D(SG1)	1.9 s
K_p	0.6 pu	D(SG2)	1.2 s

Four case studies were established with wind turbines operating an over-speed de-loading state, validated under both high and low wind condition intervals:

Case 1: Wind turbines without any supplemental control.

Case 2: Wind turbines with fixed-coefficient SVIC. The fixed parameters are set to K_d = 0.3 and K_p = 0.6 pu, which are typical values adopted in conventional SVIC strategies [10].

Case 3: Wind turbines with conventional fuzzy logic-based variable-parameter SVIC (with control coefficients independent of wind conditions variations).

Case 4: Wind turbines with parameter-adaptive SVIC (the proposed strategy).

5.1 FR Performance in High Wind Conditions Regions

The wind farm was configured to operate in the high-wind regime depicted in Fig. 5, under full-load operation without curtailment. At 333 s of simulation time, an additional 30 MW active power load was suddenly added to Load 1. The effectiveness of the four case studies in improving the system frequency was analyzed.

A comparison of the four cases in Fig. 11 and Table 5 reveals that wind turbine rotor speed varies in response to changes in wind speed. Under the no-control scenario, the turbine maintains over-speed de-loading operation (rotor velocity ≈ 1.14 p.u.) without releasing rotational kinetic energy for frequency support. The other three cases all release rotational kinetic energy to participate in system FR. When employing fixed-parameter SVIC, the constant control coefficients cannot adapt to wind condition changes. In high wind condition regions where rotational kinetic energy is abundant, this method fails to fully utilize the available kinetic energy, resulting in inferior frequency improvement compared to both variable-coefficient SVIC and the proposed adaptive control strategy.

For variable-coefficient SVIC, the control parameters are determined by fuzzy rules across the entire wind condition range. However, an excessive number of fuzzy rules leads to a significant computational burden. When the number of rules is limited, the output of the fuzzy rules becomes conservative, failing to fully utilize the rotor kinetic energy. The parameter-adaptive SVIC proposed in this paper addresses these limitations. During the initial stage of frequency disturbances when wind conditions are high and exceed the threshold, the control strategy utilizes refined fuzzy rules to dynamically adjust synthetic inertia and droop coefficients through fuzzy inference. This approach facilitates rapid inertial response, ensures maximal utilization of rotational kinetic energy, and elevates the frequency nadir. During the post-disturbance phase, the control parameters are attenuated to avoid over-depletion of kinetic energy, thereby achieving a more stable frequency recovery trajectory. The control strategy framework proposed in this paper enables wind turbines to significantly contribute to system frequency regulation in high-wind-speed regions, raising the system frequency nadir to 49.87 Hz. This represents an improvement of 31.6% and 13.3% compared to fixed-parameter SVIC and full-wind-speed fuzzy control-based variable parameter SVIC, respectively. By fully releasing rotor kinetic energy within the safe operational domain during high-wind-speed conditions, the proposed strategy allows the system to reach the frequency nadir more rapidly. Specifically, the time to reach the frequency nadir is shortened by 0.2 and 0.08 s compared to Cases 2 and 3, respectively.

Regarding the SFD phenomenon, an analysis was conducted based on Fig. 11c. The SFD is quantified as the difference between the frequency nadir and the subsequent lowest point during the recovery phase. The fixed-parameter SVIC exhibits an SFD of 0.01 Hz. In contrast, the proposed parameter-adaptive strategy results in a more pronounced SFD of 0.016 Hz. This is an expected trade-off: the aggressive energy release in Case 4 improves the primary frequency nadir by 0.06 Hz compared to Case 2, but the consequent deeper rotor deceleration requires greater power reduction during rotor speed recovery, leading to a larger SFD. The key insight is that although the proposed method produces a larger SFD magnitude, it does not create a new dangerous frequency low point. The frequency during the SFD period remains significantly higher than the primary nadir, and system stability is not compromised. Therefore, the primary design objective of maximizing inertial support to improve the critical frequency nadir has been successfully achieved. Mitigating the SFD through smooth exit strategies has been identified as a key focus for future work.

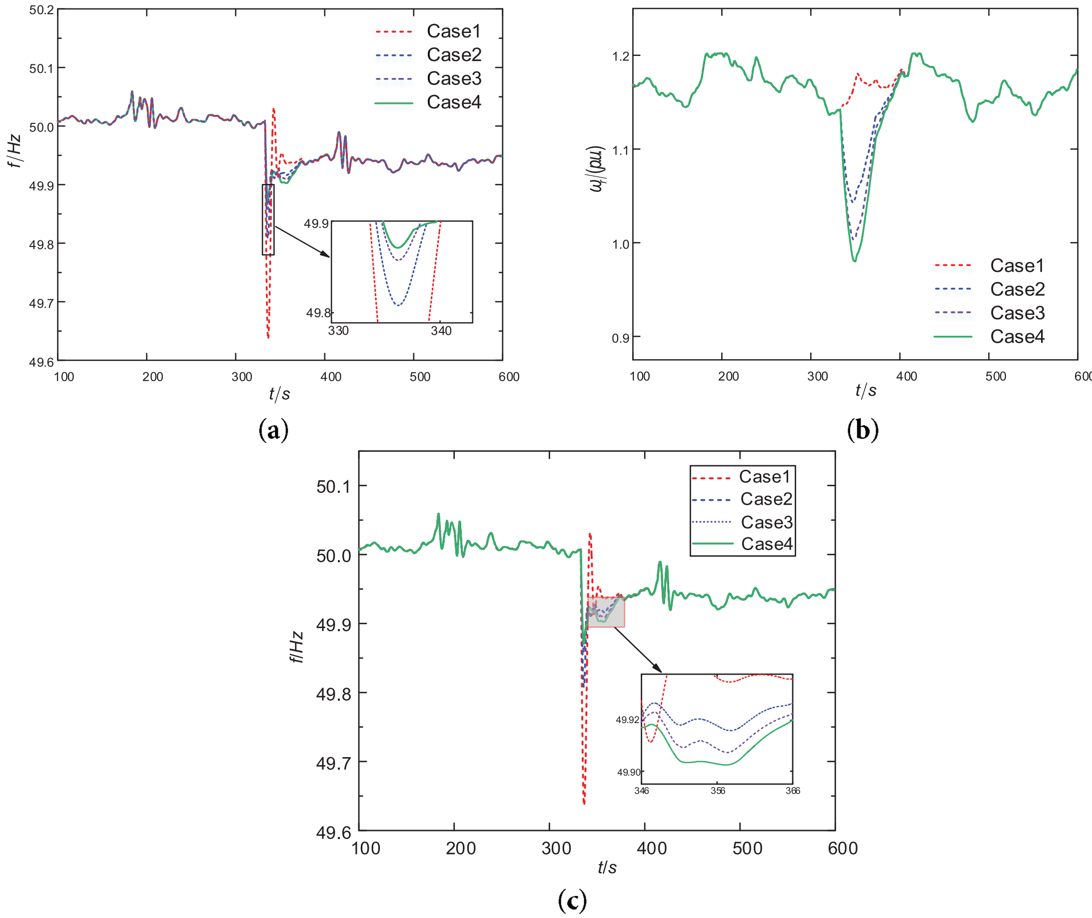

Figure 11: Simulation results under high wind conditions. (**a**) System frequency (**b**) Wind turbine rotor speed (**c**) SFD

Table 5: Simulation results table under high wind conditions

Case	Lowest frequency point (Hz)	Lowest frequency time (s)	Rotational speed (p.u.)	SFD (Hz)
Case 1	49.64	336.46	–	–
Case 2	49.81	336.22	1.05	0.01
Case 3	49.85	336.13	1.01	0.015
Case 4	49.87	336.02	0.98	0.016

5.2 FR under Low Wind Conditions

The DFIGs were configured to operate within the low wind condition regime illustrated in Fig. 5. When the simulation reached 211 s, an additional 30 MW load was suddenly added to Load 1. The effectiveness of the four cases in improving the system frequency was tested.

Under low wind conditions, the traditional SVIC maintains fixed parameters regardless of wind condition variations. During low rotor speed operation, excessively large control parameters cause wind turbines to release excessive rotational kinetic energy, resulting in rotor speed dropping below 0.7 p.u. This leads to turbine speed limit violation, as shown in Fig. 12. Since the operation below 0.7 p.u. compromises turbine safety, the frequency support capability of traditional SVIC is not considered in this analysis. The proposed control strategy in this study enables adaptive adjustment of SVIC parameters according to wind condition variations. During low wind conditions, the control parameters are reduced as wind condition decreases, ensuring that wind turbines prioritize operational safety while participating in system FR. This guarantees that the rotor speed remains within the safe operating range (above 0.7 p.u.).

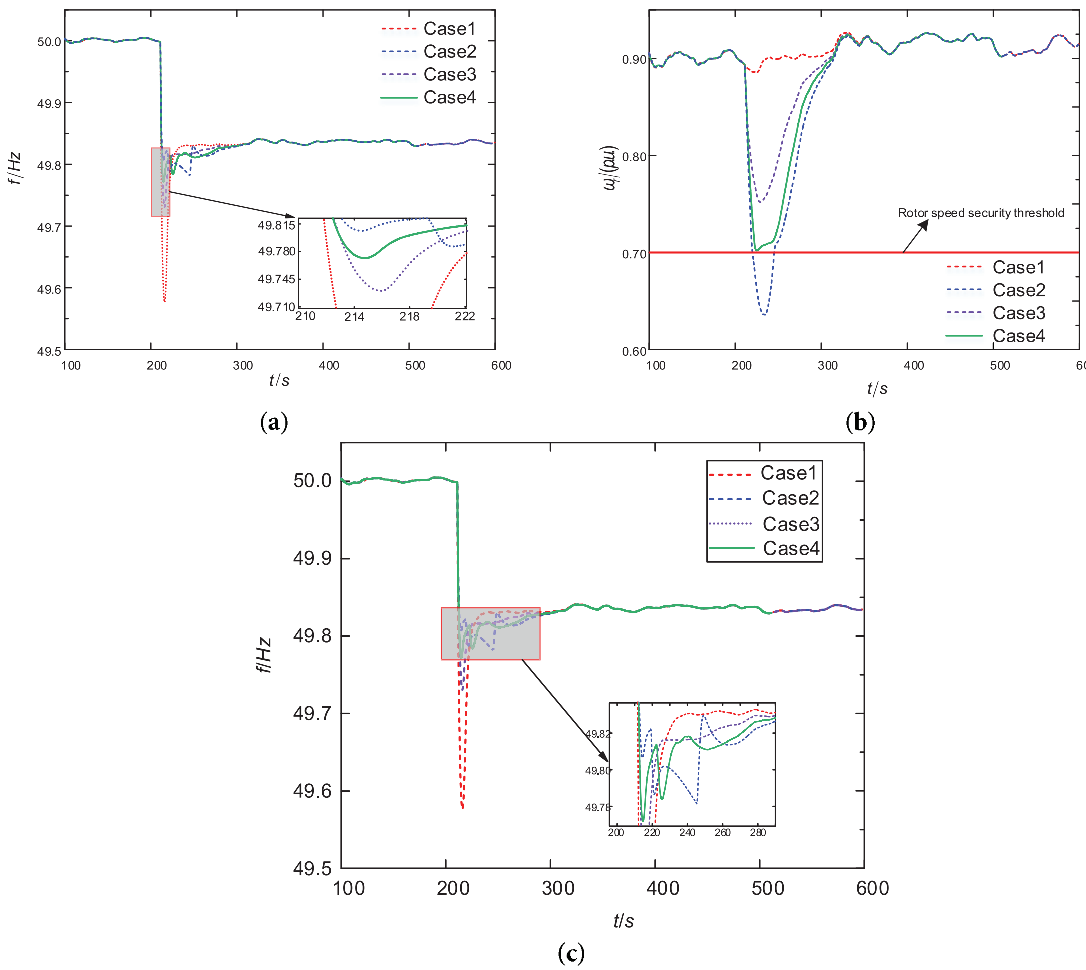

Figure 12: Simulation results under low wind conditions. (**a**) System frequency (**b**) Wind turbine rotor velocity (**c**) SFD

For the variable-coefficient SVIC utilizing fuzzy logic inference, the rule base configuration tends to yield excessively low control parameters, resulting in overly conservative control actions that lead to suboptimal frequency improvement performance. The relatively smaller control coefficients in variable-coefficient SVIC prevent excessive release of rotational kinetic energy during low wind conditions, thereby maintaining operational security. However, since this method requires establishing a comprehensive rule base across all wind condition ranges, an excessive number of rules would lead to a substantial computational burden. In contrast, the proposed control strategy not only adapts to wind conditions variations in low wind conditions but also requires lower computational resources.

While ensuring operational security of wind turbines, the proposed control strategy demonstrates superior performance during frequency events compared to other cases. It provides faster frequency response and better improvement in the frequency nadir. At low wind speeds, the adaptive framework employs a decay function to leverage the frequency regulation capability of wind turbines while ensuring rotor operational safety. The frequency nadir is improved by 21.4% compared to Case 3, as shown in Table 6.

Table 6: Simulation results table under low wind conditions

Case	Lowest frequency point (Hz)	Lowest frequency time (s)	Rotational speed (p.u.)	SFD (Hz)
Case 1	49.61	214.67	–	–
Case 3	49.72	213.96	0.73	0.01
Case 4	49.78	213.79	0.71	0.03

Regarding the SFD, the proposed control strategy prioritizes mitigating the primary frequency drop by releasing more kinetic energy, which consequently leads to a relatively larger SFD. Future work will focus on reducing the SFD by extending the rotor speed recovery time, such as through the application of logistic regression functions, integrating energy storage systems, or increasing reserve capacity.

5.3 Performance under Wind Speed Cross-Zone Condition

The preceding simulations validate the efficacy of the proposed strategy within stable high and low wind speed intervals. However, in a realistic stochastic wind environment, the wind speed frequently fluctuates around the zoning threshold. A critical concern for any zoning-based control strategy is the potential for power fluctuations or system instability during the transition between control modes. Therefore, this subsection designs a wind speed cross-zone scenario where the wind speed drops from the high-speed zone to below the threshold, explicitly testing the smoothness and robustness of the switching logic between the simplified fuzzy control and the decay-function-based control.

The initial wind speed of the wind farm was set at approximately 10 m/s (high-speed zone). At t = 62 s, the wind speed gradually decreased to around 8 m/s (low-speed zone), as shown in Fig. 13. A 30 MW load increase disturbance is applied at Load 1 at t = 58 s, ensuring the frequency event occurs while the wind turbine is operating in the high-speed zone.

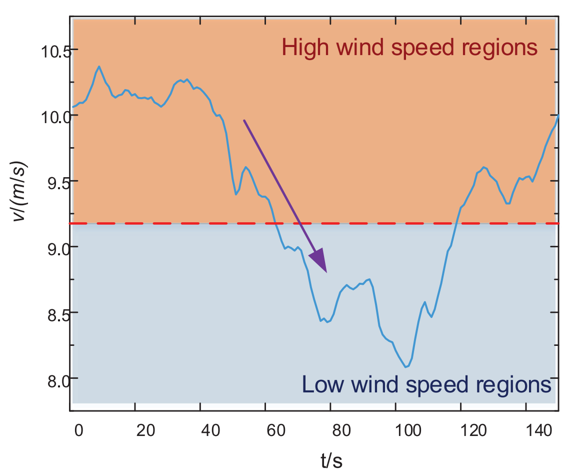

Figure 13: cross regional wind speed

The system frequency and wind turbine rotor velocity are depicted in Fig. 14.

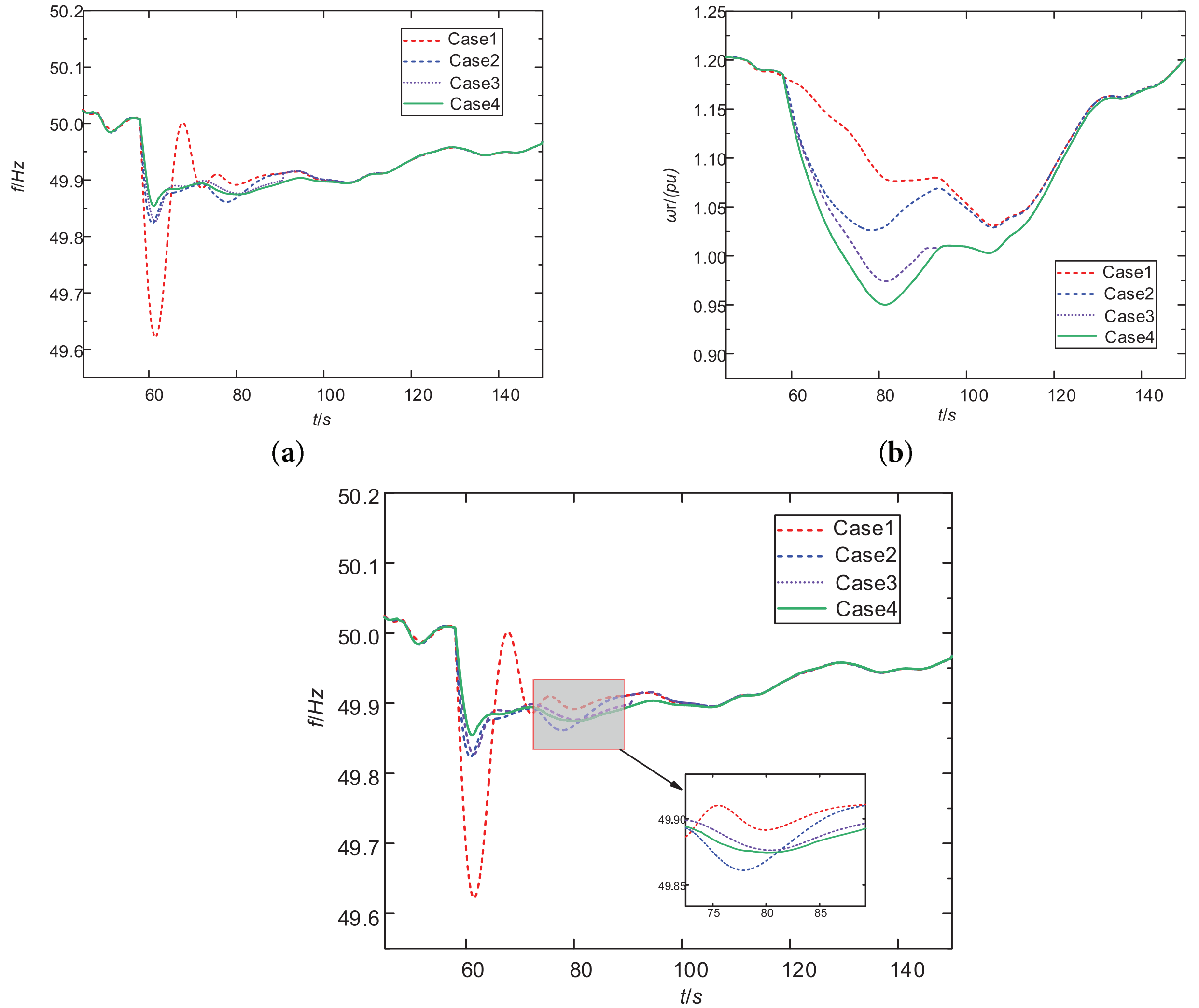

(c)

Figure 14: Simulation results under wind speed cross-zone condition. (**a**) System frequency (**b**) Wind turbine rotor velocity (**c**) SFD

Upon load increase at t = 58 s, the proposed strategy (Case 4) rapidly provides inertial support, effectively elevating the frequency nadir compared to the no-control case (Case 1). The most significant observation occurs after t = 62 s, when the wind speed drops into the low-speed zone. No abrupt change or secondary oscillation is observed in the frequency recovery trajectory. The frequency curve of Case 4 remains smooth, demonstrating that the transition between control modes is seamless and does not introduce additional disturbance to the grid.

When the doubly-fed induction generator adopts the control strategy proposed in this paper, the frequency nadir is improved by 48.7% and 11.7% compared to the scenarios with no additional control and with the traditional fuzzy control-based variable parameter control strategy, as shown in Fig. 14, respectively.

In the high-wind-speed zone, the proposed strategy employs fuzzy control-based variable-coefficient comprehensive virtual inertia control to release rotor kinetic energy within a safe range, resulting in a rotor speed decrease of 0.25 p.u., as shown in Table 7. Compared to the full-wind-speed fuzzy control-based variable-coefficient comprehensive virtual inertia control, the rotor speed decrease is 8% greater with the proposed strategy, further enhancing system frequency stability.

Table 7: Simulation results table under wind speed cross-zone condition

Case	Lowest frequency point (Hz)	Lowest frequency time (s)	Rotational speed (p.u.)	SFD (Hz)
Case 1	49.61	62.62	–	–
Case 2	49.82	60.88	1.03	0.03
Case 3	49.83	61.53	0.97	0.022
Case 4	49.85	60.47	0.95	0.020

Simulation analysis demonstrates that the adaptive control strategy based on wind speed zoning—utilizing fuzzy control in high-wind-speed regions and a decay function in low-wind-speed regions—adaptively reduces the comprehensive virtual inertia control coefficients during the frequency recovery phase. Compared to the full-wind-speed fuzzy control strategy, this approach mitigates the SFD phenomenon after the frequency regulation control concludes, achieving a relative improvement of 8.3%. In contrast, the traditional fixed-parameter comprehensive virtual inertia control exhibits a significant SFD phenomenon after the frequency regulation control ends, with frequency dropping again by 0.03 Hz, a drop of 20%. Although the proposed control strategy still exhibits a secondary frequency dip after the frequency regulation control ends, it significantly improves the frequency nadir during the primary frequency regulation process. Furthermore, by appropriately extending the rotor speed recovery time after the control strategy concludes, the impact of SFD on system frequency stability is alleviated, keeping it within safe limits.

This cross-zone simulation validates a key advantage of the proposed framework: inherent switching stability. The decision condition for mode switching is based solely on the instantaneous wind speed measurement, ensuring a deterministic and immediate transition. The decay function in the low-speed zone guarantees that the post-switch control effort is appropriate for the new, energy-limited operating condition. The results confirm that the strategy not only performs well in steady wind intervals but also maintains robust and grid-friendly operation during dynamic wind transitions, effectively mitigating concerns about control mode switching.

5.4 Discussion and Limitations

The simulation results demonstrate that the proposed wind-speed-zoning framework effectively balances FR performance and operational security. The key innovation lies not in any single component, but in the systematic integration of a simplified fuzzy logic for high-wind conditions and a dedicated decay function for low-wind conditions. This hybrid approach overcomes the fundamental limitation of prior single-strategy methods, which are forced to make compromises across the entire operating range. Our strategy allows for aggressive, high-performance control where kinetic energy is abundant, and automatically switches to a secure, conservative mode when energy is limited, thereby providing a context-aware solution.

The primary limitation of this strategy is its dependency on the predefined wind speed threshold for switching between the high and low-speed control modes. The selection of this threshold is critical: setting it too high may underutilize the available kinetic energy in medium-speed regions, while setting it too low could risk activating the aggressive fuzzy mode with insufficient rotor energy reserves. Although a reasonable threshold was determined for this study, its optimal value may vary with specific turbine characteristics and grid requirements. Therefore, future work will focus on developing adaptive methods to dynamically optimize this switching threshold, further enhancing the strategy's robustness and performance across diverse operational scenarios.

6 Conclusion

To address the kinetic energy security constraints of DFIGs during FR under stochastic wind scenarios, this paper proposes a coordinated strategy integrating fuzzy parameter adaptation with over-speed de-loading. The following conclusions are drawn:

(1) Traditional SVIC employs fixed control coefficients, which leads to insufficient utilization of rotor kinetic energy under high wind conditions, and risks rotor speed excursions under low wind conditions. Additionally, the withdrawal of control post-FR tends to induce SFD.
(2) A wind condition-frequency dual-mode fuzzy logic framework is established. Under high wind conditions, it fully exploits the rotor kinetic energy, while under low wind conditions, a wind condition-adaptive control parameter attenuation mechanism is implemented to ensure rotor speed security.
(3) The proposed strategy significantly enhances computational efficiency while ensuring FR performance. By adopting simplified fuzzy rules in high wind condition zones, the computational burden is reduced by approximately 40% compared to variable-coefficient virtual inertia control across the full wind condition range.

Acknowledgement: None.

Funding Statement: The National Natural Science Foundation of China (52477178).

Author Contributions: The authors confirm contribution to the paper as follows: Conceptualization, Methodology: Li Sun, Fanjun Zeng and Hongbo Liu; Validation, Writing—original draft preparation: Fanjun Zeng; Supervision, Funding acquisition: Chenglian Ma; Writing—review and editing: Li Sun; Data curation, Visualization: Qiting Zhang; Formal analysis, Investigation: Qiting Zhang and Jingzhou Zhu. All authors reviewed the results and approved the final version of the manuscript.

Availability of Data and Materials: Data that support the findings of this study are included within the article.

Ethics Approval: Not applicable.

Conflicts of Interest: The authors declare no conflicts of interest to report regarding the present study.

Nomenclature

SVIC	Synthetic virtual inertia control
DFIG	Doubly-fed induction generator
FR	Frequency regulation
MPPT	Maximum power point tracking
PD	Proportional-derivative
RoCoF	Rate of change of frequency
FIS	Fuzzy inference system
FLC	Fuzzy logic controller
SFD	Second frequency drop

References

1. Prabhakar K, Jain SK, Padhy PK. Inertia estimation in modern power system: a comprehensive review. Electr Power Syst Res. 2022;211(1):108222. doi:10.1016/j.epsr.2022.108222.
2. Liu Z, Tian M. Analyzing frequency characteristics: the role of traditional and virtual inertia in power systems. In: Proceedings of the 2024 8th International Conference on Electrical, Mechanical and Computer Engineering (ICEMCE); 2024 Oct 25–27; Xi'an, China. p. 215–9. doi:10.1109/ICEMCE64157.2024.10862086.
3. Xue S, Yang Z, Yin Z, Yu F, Wang Z. The frequency regulation scheme of a wind turbine generator based on variable tracking operation. Electronics. 2024;13(13):2575. doi:10.3390/electronics13132575.
4. Fradley J, Preece R, Barnes M. The influence of network factors on frequency stability. IEEE Trans Power Syst. 2020;35(4):2826–34. doi:10.1109/TPWRS.2019.2958842.
5. Wu YK, Chang SM, Hu YL, Hsu WH, Lan BR. FR technologies from a single wind turbine or wind farm. In: Proceedings of the 2018 IEEE International Conference on Applied System Innovation (ICASI); 2018 Apr 13–17; Chiba, Japan. p. 1240–3. doi:10.1109/ICASI.2018.8394515.
6. Fernández-Guillamón A, Muljadi E, Molina-García A. Frequency control studies: a review of power system, conventional and renewable generation unit modeling. Electr Power Syst Res. 2022;211:108191. doi:10.1016/j.epsr.2022.108191.
7. Tu G, Li Y, Xiang J. Coordinated rotor speed and pitch angle control of wind turbines for accurate and efficient frequency response. IEEE Trans Power Syst. 2022;37(5):3566–76. doi:10.1109/TPWRS.2021.3136822.
8. Yue X, Cai Z, Luo Z, Li X, Liu R, Zhu F. A kind of variable pitch control of wind turbine based on fuzzy control under extreme wind conditions. In: Proceedings of the 2023 3rd New Energy and Energy Storage System Control Summit Forum (NEESSC); 2023 Sep 26–28; Mianyang, China. p. 195–8. doi:10.1109/NEESSC59976.2023.10349312.
9. Mohanty D, Giri A, Panda S. Frequency regulation by optimized fuzzy based self-adaptive virtual inertia control for microgrid with variable renewable penetration. J Energy Storage. 2024;104:114433. doi:10.1016/j.est.2024.114433.
10. Li KX, An J, Shi Y, Zhou YB, Liu CY. An integrated virtual inertia control parameter setting method for wind turbine based on available FR energy. Trans China Electrotech Soc. 2025;40(5):1382–94. (In Chinese). doi:10.19595/j.cnki.1000-6753.tces.240400.
11. Li Q, Ren B, Li Q, Wang D, Tang W, Meng J, et al. Virtual inertial control strategy based on fuzzy logic algorithm for PMSG wind turbines to enhance frequency stability. Front Energy Res. 2022;10:907770. doi:10.3389/fenrg.2022.907770.
12. Jiang Y, Wang C, Xiao L, Yu D, Zhang X. Wind/storage coordinated control strategy based on system frequency regulation demands. Energy Rep. 2024;11:1551–9. doi:10.1016/j.egyr.2024.01.002.
13. Ma D, Li W. Wind-storage combined virtual inertial control based on quantization and regulation decoupling of active power increments. Energies. 2022;15(14):5184. doi:10.3390/en15145184.
14. Morren J, de Haan SWH, Kling WL, Ferreira JA. Wind turbines emulating inertia and supporting primary frequency control. IEEE Trans Power Syst. 2006;21(1):433–4. doi:10.1109/TPWRS.2005.861956.
15. Gao H, Zhang F, Ding L, Cornélusse B, Zhang G, Salimu A. Multi-segment droop control and optimal parameter setting strategy of wind turbine for frequency regulation. Int J Electr Power Energy Syst. 2024;158:109968. doi:10.1016/j.ijepes.2024.109968.
16. Li Z, Yang L, Xu Y. A dynamics-constrained method for distributed frequency regulation in low-inertia power systems. Appl Energy. 2023;344:121256. doi:10.1016/j.apenergy.2023.121256.
17. Ding X, Zhang Y. Adaptive virtual inertia in doubly fed induction generators for enhanced frequency regulation. IEEE Access. 2025;13:55616–26. doi:10.1109/ACCESS.2025.3555443.
18. Ke X, Zhang W, Li P, Niu S, Sheng S, Yang J. Fuzzy adaptive virtual inertia control for high wind power penetration system. Power Syst Technol. 2020;44(6):2127–36. (In Chinese). doi:10.13335/j.1000-3673.pst.2019.1349.
19. Li JH, Song CX, Lan F. Optimal control strategy of virtual inertia for wind turbine based on fuzzy inference of parameters. Autom Electr Power Syst. 2023;47(20):125–33. (In Chinese). doi:10.7500/AEPS20220913008.
20. Li BK, Zhang F, Ding L. Fuzzy cooperative control and parameter correction strategy of speed controller in frequency modulation stage of doubly-fed induction generator. Power Syst Technol. 2022;46(2):596–605. (In Chinese). doi:10.13335/j.1000-3673.pst.2021.0358.

21. Ding L, Yin SY, Wang TX, Jiang JP, Cheng FM, Si JC. Integrated frequency control strategy of DFIGs based on virtual inertia and over-speed control. Power Syst Technol. 2015;39(9):2385–91. (In Chinese). doi:10.13335/j.1000-3673.pst.2015.09.002.
22. Wang Y, Guo Y, Chen Y, Xu W. Analysis of frequency regulation capability and fatigue loads of wind turbine based on over-speed control. Electronics. 2023;12(9):2009. doi:10.3390/electronics12092009.
23. Attya ABT, Dominguez-García JL. Insights on the provision of frequency support by wind power and the impact on energy systems. IEEE Trans Sustain Energy. 2018;9(2):719–28. doi:10.1109/TSTE.2017.2759503.
24. Zhang X, Zha X, Yue S, Chen Y. A FR strategy for wind power based on limited over-speed de-loading curve partitioning. IEEE Access. 2018;6:22938–51. doi:10.1109/ACCESS.2018.2825363.
25. Hu Y, Wang Z, Huang T, Zeng Q. A novel frequency response analysis model applicable to high-penetration wind power grid. Energy Rep. 2022;8(1):412–21. doi:10.1016/j.egyr.2022.08.097.